

Optimization of AC Parameters for Efficient Heating and Minimal Capacity Loss in Lithium-Ion Batteries

Jun Li¹, Zixian Zhuang¹, Weiling Luan^{1*}, Haofeng Chen^{12*}

1 Key Laboratory of Advanced Battery Systems and Safety (CPCIF), School of Mechanical and Power Engineering, East China University of Science and Technology, Shanghai 200237, P. R. China

2 Department of Mechanical & Aerospace Engineering, University of Strathclyde, Glasgow G1 1XJ, UK

(*Corresponding Author: luan@ecust.edu.cn, haofeng.chen@ecust.edu.cn)

ABSTRACT

Lithium-ion batteries have played a significant role in industries such as new energy vehicles. However, the performance of lithium-ion batteries is seriously affected by low temperatures. Alternating current (AC) self-heating is a feasible method to eliminate the negative effects of low temperatures on lithium-ion batteries. Nevertheless, the capacity degradation of batteries can be generated if the amplitude and frequency of AC are not adopted properly. In this study, the boundaries of temperature rise and capacity loss are calculated by an electrochemical-thermal coupled (ETC) model verified by experiments, and the range of AC parameters that satisfies the temperature rise requirement without capacity loss is determined. This range of AC parameters results from a combination of high amplitude and high frequency. Using AC in the range can heat the battery from -20 °C to above 0 °C within 5 minutes without any capacity loss.

Keywords: lithium-ion battery, self-heating, electrochemical-thermal coupled model, temperature rise, capacity loss

E_a	Activation energy
F	Faraday constant
R	Ideal gas constant
T_0	Environmental temperature
T_r	Reference temperature
T	Battery temperature
φ_{DL}	Double layer overpotential
φ_{pla}	Lithium plating overpotential
C_{nel}	Liquid phase concentration
C_p	Battery specific heat capacity
h	Convective heat transfer coefficient
$i_{0,pla}$	Lithium plating exchange current density
i_{DL}	Double layer current density
$i_{Li,int}$	Lithium intercalation current density
$i_{Li,pla}$	Lithium plating current density
i_{sum}	Electrode current density
k_{pla}	Lithium plating reaction rate constant
Q_j	Heat source
α_{pla}	Lithium plating transfer coefficient
ρ	Battery density

NONMENCLATURE

Abbreviations

AC	Alternating Current
ETC	Electrochemical-Thermal Coupled
P2D	Pseudo-Two-Dimensional

Symbols

A	Heat transfer surface area
Arrhe	Temperature correction coefficient
C_{DL}	Double layer capacitor

1. INTRODUCTION

Lithium-ion batteries have been widely used in various fields such as mobile devices, electric vehicles, energy storage, and renewable energy due to their advantages of high energy density, reusability, and environmental friendliness [1]. However, low temperatures can critically affect the charging and discharging performance of lithium-ion batteries, resulting in an increase in internal resistance and a decrease in capacity [2]. More seriously, lithium plating from low temperature charging not only gives rise to irreversible capacity degradation, but lithium dendrites

can also cause internal short circuits, causing serious safety accidents [3, 4]. Therefore, it is necessary to keep the battery at a mild operating temperature to eliminate the negative effects of low temperature.

Pre-heating the batteries before use emerges is a viable approach. Battery pre-heating techniques can be categorized into external heating and internal self-heating methods based on different heat sources [5-8]. The self-heating method is a highly valuable heating approach achieved by applying AC to the battery and utilizing the heat generated by the battery's own impedance to warm itself. Self-heating does not rely on additional heating equipment and provides better heat uniformity [9]. However, improper adjustments in self-heating amplitude and frequency can potentially result in battery capacity degradation [10, 11]. Currently, the lack of quantitative analysis in existing studies regarding the impact of self-heating parameters on battery capacity degradation makes it challenging to optimize self-heating effectively. Therefore, it is essential to determine suitable self-heating parameters that strike a balance between temperature rise and capacity degradation.

In this study, an ETC model incorporating lithium plating reactions and double-layer effects is established. This model accurately captures battery responses under high-frequency current excitation. The model is validated experimentally under different AC amplitudes and frequencies, accurately predicting temperature rise and capacity degradation during low-temperature AC self-heating. Based on the ETC model, the boundaries of AC parameters for battery temperature rise and capacity loss are calculated. The determination of two boundaries provides rational recommendations for the selection of AC parameters.

2. ESTABLISHMENT OF ETC MODEL

Doyle and Newman developed a P2D model, which incorporates charge conservation and mass conservation equations in the solid and liquid phases of the lithium-ion battery, as well as electrochemical reaction rate equations at the solid-liquid interface. Solving this model enables an accurate analysis of the distribution states and dynamic processes of charges and lithium ions within the battery.

The traditional P2D model is established under the isothermal assumption. To calculate the temperature variation of the battery, the Arrhenius equation is used to couple temperature and electrochemical parameters, as shown in Eq. (1). The temperature of batteries is

calculated using the energy conservation equation, as shown in Eq. (2).

$$Arrhe = \exp\left[\frac{E_a}{R}\left(\frac{1}{T_r} - \frac{1}{T}\right)\right] \quad (1)$$

$$\rho c_p \frac{\partial T}{\partial t} = q_j - hA(T - T_0) \quad (2)$$

Under low-temperature AC conditions, the lithium plating reaction on the negative electrode surface is the primary cause of battery capacity degradation. This process can be described using the Butler-Volmer equation. The current density and exchange current density for the lithium plating reaction are shown in Eqs. (3) and (4).

$$i_{Li,pla} = i_{0,pla} \left[\exp\left(\frac{\alpha_{pla}\phi_{pla}F}{RT}\right) - \exp\left(\frac{(1-\alpha_{pla})\phi_{pla}F}{RT}\right) \right] \quad (3)$$

$$i_{0,pla} = Fk_{pla}c_{hel}^{\alpha_{pla}} \quad (4)$$

When the amplitude and direction of the current change frequently, the double layer on the surface of electrode active particles needs to be taken into consideration. The double layer current density can be represented by Eq. (5).

$$i_{DL} = C_{DL} \frac{\partial \phi_{DL}}{\partial t} \quad (5)$$

Consequently, the total local current density at the negative electrode surface can be expressed by Eq. (6). In contrast, at the positive electrode surface, only lithium-ion intercalation/deintercalation reactions and the double layer exist.

$$i_{sum} = i_{Li,int} + i_{Li,pla} + i_{DL} \quad (6)$$

3. SELF-HEATING EXPERIMENT

In this study, LFP 18650 batteries were used to validate the accuracy of the ETC model. The experimental setup mainly consists of a high-low temperature test chamber for providing a low-temperature environment, a bipolar power supply for delivering high-frequency AC, an intelligent battery cycling equipment for testing battery capacity, and a

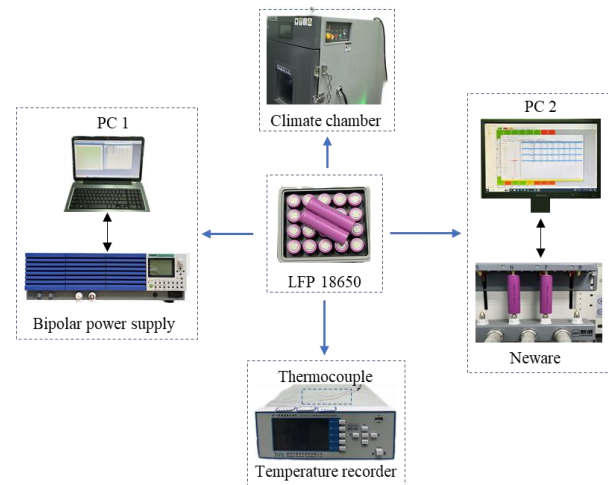


Fig. 1. Low-temperature AC self-heating experimental platform

multi-channel temperature recorder for temperature acquisition and recording, as illustrated in Fig. 1.

4. RESULTS AND DISCUSSION

4.1 Model validation

Temperature and capacity loss of the batteries after five minutes of self-heating in a -20 °C environment were obtained through experimental and simulation approaches. Fig. 2 shows the comparisons of experiment and simulation for temperature rise under various AC parameters. In Fig. 2, solid lines represent simulated data, while dashed lines represent experimental data. It can be observed that the simulated results match well with the experimental data. Measurements of battery capacity changes were conducted after 60 heating cycles under various AC parameters. The comparisons of the experiment and simulation for capacity loss are shown in the Table 1.

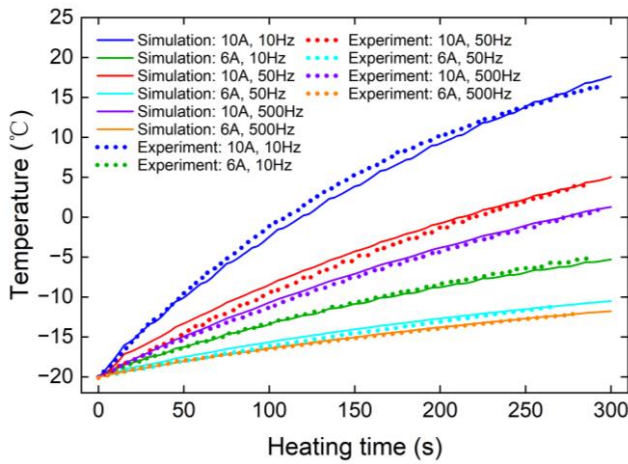


Fig. 2. Comparison of temperature rise between simulation and experiment

Table 1. Comparison of capacity loss between simulation and experiment

AC parameters	Capacity loss	
	Experiment	Simulation
10 A, 10 Hz	407.65	391.04
6 A, 10 Hz	234.72	211.45
10 A, 50 Hz	74.58	61.99
6 A, 50 Hz	19.03	10.24
10 A, 500 Hz	0	0
6 A, 500 Hz	0	0

A preliminary analysis of temperature rise and capacity loss under different AC parameters reveals that with larger AC amplitudes and lower frequencies, the battery experiences a faster temperature rise and greater capacity loss. When the AC frequency increases to a certain extent, the battery will no longer undergo capacity loss.

4.2 Analysis of temperature rise and aging

Based on the previous analysis, the realization of fast temperature rise and low capacity loss during self-heating of the battery conflicts with each other. High AC amplitude and low AC frequency are required to achieve fast temperature rise, while low AC amplitude and high AC frequency are required to reduce capacity loss. Hence, there are certain combinations of AC parameters that can achieve both objectives simultaneously.

To identify AC parameters that can simultaneously satisfy the temperature rise requirements without capacity loss, the entire AC parameter space is explored using the ETC model, which can calculate battery temperature rise and capacity loss. The range of the AC parameter space is initially defined. According to Li et al. [12], vehicle batteries can use the battery's own power to heat themselves. The specific method is converting the battery's own direct current into AC through the action of the vehicle's motor, thereby achieving self-heating. Therefore, the upper limit of the AC frequency is set to 1000 Hz. Furthermore, excessively high AC amplitudes may exceed the battery's capacity, potentially leading to safety incidents. Therefore, the upper limit of the battery's AC amplitude is set at 12A. In conclusion, the parameter space for AC is as follows:

$$\text{Amplitude} \in [0,12] \text{ (A)} \quad (7)$$

$$\text{Frequency} \in [10,1000] \text{ (Hz)} \quad (8)$$

The purpose of AC self-heating is to elevate the battery's temperature and prevent adverse effects from low temperatures. Although low AC amplitudes and high AC frequencies can prevent capacity loss, they may not sufficiently raise the battery's temperature to the required level. For LFP batteries, the performance significantly deteriorates when the temperature drops below 0 °C. Hence, the battery temperature needs to reach 0 °C after heating to satisfy the requirements. As a result, setting the AC parameters that can heat the battery to 0 °C as the boundary of temperature rise for the battery. Based on the previous analysis, when the AC parameters reach a certain level, the battery does not experience capacity degradation. Using the AC parameters that exactly prevent capacity loss as the boundary of capacity loss for the battery.

Under the above conditions, the boundary of battery temperature rise and capacity loss calculated using the ETC model are shown in Fig. 3. The initial heating temperature of the battery is -20 °C and the heating time is 5 minutes. Plot 3D cloud chart with frequency on the x-axis, amplitude on the y-axis, and battery temperature (T_{bat}) and capacity loss (Q_{loss}) after AC self-heating on the z-axis. In Fig. 3(a), the yellow line represents the AC

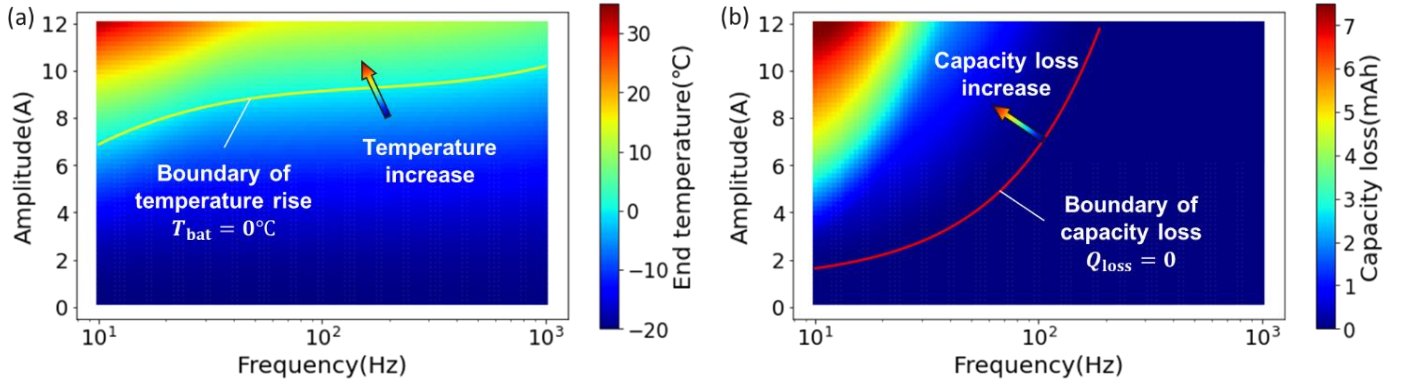


Fig. 3. Cloud charts and boundaries of battery (a) temperature and (b) capacity loss after 5 minutes of AC self-heating

parameters that can heat the battery to 0 °C and is also referred to as the boundary of temperature rise. Above the boundary curve of temperature rise, T_{bat} is greater than 0 °C, and the further away from the boundary, the higher the T_{bat} . Below the boundary curve of temperature rise, T_{bat} is less than 0 °C, and the further away from the boundary, the lower the T_{bat} . In Fig. 3(b), the red line represents the AC parameters that are just right to avoid capacity loss and is also referred to as the boundary of capacity loss. Above the boundary curve of capacity loss, Q_{loss} is greater than 0, and the further away from the boundary, the higher the Q_{loss} . Below the boundary curve of capacity loss, Q_{loss} equals to 0.

To visually represent the relationship between frequency, amplitude, temperature, and capacity loss more intuitively, a 4-D relationship chart was created. In Fig. 4, frequency is on the x-axis, amplitude is on the y-axis, capacity loss is on the z-axis, and temperature is

be satisfied within the AC parameter space composed of high frequency and high amplitude.

Simultaneously plot the boundary of temperature rise and capacity loss within the AC parameter space, as shown in Fig. 5. It can be observed that the two boundaries divide the AC parameter space into four regions:

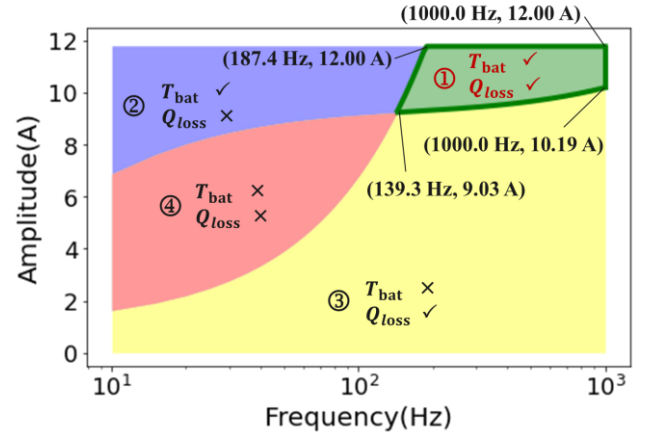


Fig. 5. AC parameter space partition

Region 1: Using the AC parameters from Region 1 to heat the battery for 5 minutes, the temperature can rise to above 0 °C without capacity loss.

Region 2: Using the AC parameters from Region 2, the temperature can rise to above 0 °C, but the capacity will be lost.

Region 3: Using the AC parameters from Region 3, the temperature cannot reach 0 °C, but the capacity will not be lost.

Region 4: Using the AC parameters from Region 4, the temperature cannot reach 0 °C, and the capacity will be lost.

Therefore, using the AC parameters from Region 1 can satisfy the basic temperature rise requirements, and the battery capacity will not be lost during the self-heating. Convert the boundaries of Region 1 into expressions as shown in Eq. (9):

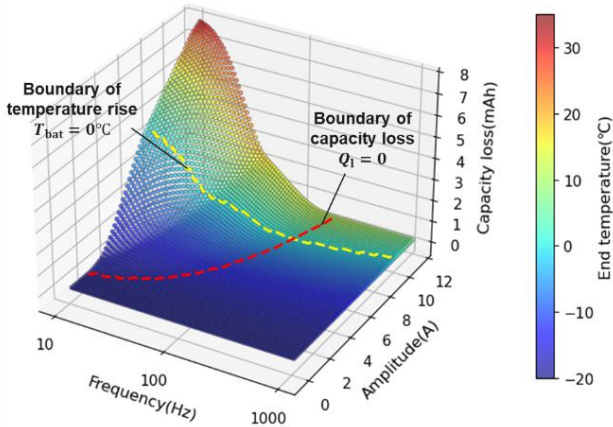


Fig. 4. 4-D relationship chart of frequency, amplitude, battery temperature and capacity loss after 5 minutes of AC self-heating

represented by different colors. It can be observed that high temperature and low capacity loss are conflicting under most AC parameters. The requirements can only

$$\left\{ \begin{array}{l} 0.9508 (\log_{10} \text{Freq})^3 - 6.309 (\log_{10} \text{Freq})^2 \\ + 14.53 \log_{10} \text{Freq} - 2.293 - A_m \leq 0 \\ 0.0572 \text{Freq} + 1.056 - A_m \geq 0 \\ A_m \leq 12 \\ \text{Freq} \leq 1000 \end{array} \right. \quad (9)$$

5. CONCLUSIONS

In this study, an ETC model was established to calculate the temperature rise and capacity loss of the battery, aiming at the problem of capacity degradation caused by improper selection of AC frequency and amplitude during self-heating. Firstly, through experiments and simulations, it is found that AC of high amplitude and low frequency will increase the temperature rise rate of the battery, but will lead to the loss of battery capacity. The goals of rapid temperature rise and low capacity loss are contradictory. Then the boundaries of temperature rise and capacity loss of the battery are determined by using the ETC model to traverse the AC parameter space. The boundaries of temperature rise and capacity loss divide the AC parameter space into four regions, and only high frequency and high amplitude AC parameters can heat the battery to above 0 °C within 5 minutes without capacity loss.

ACKNOWLEDGEMENT

The authors gratefully acknowledge the support from the National Natural Science Foundation of China (52375144, 52130511, 52150710540 and 52375145) and the East China University of Science and Technology, University of Strathclyde during the course of this work.

DECLARATION OF INTEREST STATEMENT

The authors declare that they have no known competing financial interests or personal relationships that could have appeared to influence the work reported in this paper. All authors read and approved the final manuscript.

REFERENCE

- [1] Xu JJ, Cai XY, Cai SM, et al. High-energy lithium-ion batteries: Recent progress and a promising future in applications. *Energy Environ Mater* 2023;6(5).
- [2] Bandhauer TM, Garimella S, Fuller TF. A critical review of thermal issues in lithium-ion batteries. *J Electrochem Soc* 2011;158(3):R1-R25.
- [3] Feng XN, Ouyang MG, Liu X, et al. Thermal runaway mechanism of lithium ion battery for electric vehicles: A review. *Energy Storage Mater* 2018;10:246-67.

[4] Wu SM, Wang C, Luan WL, et al. Thermal runaway behaviors of li-ion batteries after low temperature aging: Experimental study and predictive modeling. *J Energy Storage* 2023;66,107451.

[5] Wang YJ, Zhang XC, Chen ZH. Low temperature preheating techniques for lithium-ion batteries: Recent advances and future challenges. *Appl Energy* 2022;313,118832.

[6] Zhang XH, Li Z, Luo LA, et al. A review on thermal management of lithium-ion batteries for electric vehicles. *Energy* 2022;238,121652.

[7] Zhang JB, Ge H, Li Z, et al. Internal heating of lithium-ion batteries using alternating current based on the heat generation model in frequency domain. *J Power Sources* 2015;273:1030-7.

[8] Wu XG, Cui ZH, Chen ES, et al. Capacity degradation minimization oriented optimization for the pulse preheating of lithium-ion batteries under low temperature. *J Energy Storage* 2020;31,101746.

[9] Ji Y, Wang CY. Heating strategies for li-ion batteries operated from subzero temperatures. *Electrochim Acta* 2013;107:664-74.

[10] Zhu JG, Sun ZC, Wei XZ, et al. An alternating current heating method for lithium-ion batteries from subzero temperatures. *Int J Energy Res* 2016;40(13):1869-83.

[11] Li JQ, Sun DN, Chai ZX, et al. Sinusoidal alternating current heating strategy and optimization of lithium-ion batteries with a thermo-electric coupled model. *Energy* 2019;186,115798.

[12] Li Y, Gao X, Qin Y, et al. Drive circuitry of an electric vehicle enabling rapid heating of the battery pack at low temperatures. *iScience* 2021;24(1):101921.